http://periodicos.sbu.unicamp.br/ojs/index.php/parc
http://dx.doi.org/10.20396/parc.v13i00.8665827

THE EFFECTS OF CLIMATE CHANGE ON URBAN THERMAL COMFORT CONDITIONS

OS EFEITOS DAS MUDANÇAS CLIMÁTICAS NAS CONDIÇÕES DE CONFORTO TÉRMICO URBANO

Layra Ramos Lugão [1]

Juliana Silva Almeida Santos [2]

Anderson Azevedo Fraga [3]

Edna Aparecida Nico Rodrigues [4]

Cristina Engel de Alvarez[5]

[1] Universidade Federal do Espírito Santo, Vitória, ES, Brasil, layra.lugao@aluno.ufes.br
2 Universidade Federal do Espírito Santo, Vitória, ES, Brasil, jsantos.mestrado@gmail.com
3 Universidade Federal do Espírito Santo, Vitória, ES, Brasil, anderson.fraga@aluno.ufes.br
4 Universidade Federal do Espírito Santo, Vitória, ES, Brasil, edna.rodrigues@ufes.br
5 Universidade Federal do Espírito Santo, Vitória, ES, Brasil, cristina.engel@ufes.br

Authors' contribution:
LRL: conceptualization, data curation, methodology, visualization, writing - original draft, writing - review and editing, investigation. **JSAS**: conceptualization, methodology, visualization, writing - original draft, writing - review and editing, investigation. **AAF**: conceptualization, methodology, visualization, writing - original draft, writing - review and editing, investigation. **EANR**: project management, writing - proofreading and editing. **CEA**: project management, supervision, writing - proofreading and editing.

Funding: Coordination for the Improvement of Higher Education Personnel.
Conflict declaration: nothing has been declared.

Responsible Editor:
Sidney Piochi Bernardini

Abstract

Climate change is a global reality, leading to consequences for both the natural and urban environment. These changes and their implications can be perceived in features such as ecological cycles, in the economic status of a country, or on the well-being and physical integrity of a population. Hence, this study aimed to analyse the effects of climate change on urban thermal comfort and the physiological limits of a population in a tropical city, applying the Physiological Equivalent Temperature (PET) index and correlating it to the local wet-bulb temperature. The method adopted consists of four stages: (1) assembling weather files for future scenarios; (2) setting up scenarios for computational simulations; (3) choosing the most adequate urban thermal comfort index; and (4) selecting a risk parameter to evaluate human health risk. The results show that the presumed urban temperatures, considering 2050 and 2080 scenarios as parameters, can cause serious damage to inhabitants' health, given the frequency of high temperatures recorded in some months of the year. Accordingly, it is clear that there is a need for balance between the temperature variables and relative air humidity is required, striving for better comfort conditions, as well as improving users' permanence in external environments.

Keywords: climate change, heat island, urban thermal comfort, human thermoregulation, PET.

Resumo

As mudanças climáticas são uma realidade mundial, trazendo consequências tanto para o ambiente natural como urbano. As implicações das alterações do clima trazem impactos nos ciclos ecológicos, na economia, e também na integridade física e no bem-estar da população. O objetivo desta pesquisa foi analisar o efeito das mudanças climáticas na condição de conforto térmico no meio urbano considerando os limites fisiológicos da população em uma cidade de clima tropical, a partir da aplicação do índice PET (Physiological Equivalent Temperature) correlacionado à TBU (Temperatura de Bulbo Úmido). Para tal, o método adotado foi estabelecido a partir de quatro etapas: (1) preparação dos arquivos climáticos futuros; (2) definição dos cenários para simulação; (3) seleção do índice de conforto térmico urbano; e (4) definição do parâmetro para avaliação de risco para a saúde humana. Os resultados alcançados demonstram que as temperaturas presumidas para o meio urbano no recorte territorial considerado, tendo por parâmetros de análise o cenário atual e os previstos para 2050 e 2080, podem causar sérios riscos à saúde dos transeuntes, especialmente em alguns meses do ano. Por conseguinte, evidencia-se a necessidade de equilíbrio das variáveis de temperatura e umidade relativa do ar, visando a ampliação das condições de conforto e incentivo à permanência dos usuários em meios externos.

Palavras-chave: mudanças climáticas, ilha de calor, conforto térmico urbano, termorregulação humana, PET.

How to cite this article:

LUGÃO, L. R.; SANTOS, J. S. A.; FRAGA, A. A.; NICO-RODRIGUES, E. A.; ALVAREZ, C. E. de. The effects of climate change on urban thermal comfort conditions. **PARC Pesq. em Arquit. e Constr.**, Campinas, SP, v. 13, p. e022022, 2022. DOI: http://dx.doi.org/10.20396/parc.v13i00.8665827

Submitted 31;05;2021 – Approved 22.11.2021 – Published 27.06.2022

Introduction

Climate change poses a great risk to ecosystems that constantly depend on the thermal balance of the planet (LAPOLA *et al*., 2019). Among the large-scale climate forecasts, extreme weather events are considered to have a great impact given the potential to intensify other specific events, such as the influence of heat waves in inducing forest fires. In 2020, at the end of a severe drought that led to large agricultural losses, this scenario could be observed in parts of Brazil, where some cities recorded their hottest days, recording temperatures of up to 44.6°C (WMO, 2020).

An increase in the average temperature variability is foresee for tropical regions, which are more susceptible to heat waves and extreme temperatures, with a progressive amount of hotter days in pessimistic scenarios. Particularly in developing countries, this thermal trend sets tropical cities to a worsening imbalance between social, economic and environmental aspects (BATHIANY *et al*., 2018; FERON *et al*., 2019).

Due to the heat island phenomenon, urban areas, especially, tend to have higher temperatures than rural areas and climate impacts can further aggravate this condition. The health of the urban population can be strongly influenced as high temperatures and strong solar radiation cause photochemical reactions responsible for the emission of polluting gases and particles into the atmosphere (RIBEIRO; SANTOS, 2016). Thus, the U.S. Environmental Protection Agency and Centers for Disease Control and Prevention (CLIMATE, 2016) point out three stages of the most common health symptoms caused by extreme heat: cramps, exhaustion and heat stroke. These reactions often affect the body's ability to maintain a mean temperature, especially in vulnerable groups such as children, the elderly and people with pre-existing illnesses.

In order to verify environmental conditions at different urban scales, different methodologies have been developed to address external thermal comfort index (MAUREE *et al.*, 2019). One of these indices is the Physiological Equivalent Temperature (PET), which associates climatic parameters to the human thermoregulatory process, considering clothing and activities performed in a thermal sensation assessment (HÖPPE, 1999). PET temperatures are determined by the unit (°C), facilitating handling by urban planners who are unfamiliar with human biometeorology (MATZARAKIS; MAYER; IZIOMON, 1999).

Thermal comfort ranges were initially developed in temperate regions, thus the PET temperature ranges had to be calibrated for the location to be evaluated (SILVA; ALVAREZ, 2015). Considering the existing climate diversity and individual particularities related to thermal preferences, climate variables were monitored *in loco,* associated with surveys to inquire population about its thermal sensation (KRÜGER *et al*. 2018).

According to Raymond, Matthews and Horton (2020), for an adequate analysis of the physiological risk of the population in outdoor environments, it is essential to evaluate the Wet-Bulb Temperature (WBT) variable. Sherwood and Huber (2010) found that there is a limit to the human body´s ability to adapt to heat and humidity stress, represented by a WBT greater than 35°C. When the human body is exposed to a level above this limit for a long period, heat dissipation becomes physically impossible as the body's thermoregulation is conditioned to a climatic limit (SCHÄR, 2016).

Given the scenario of global warming in cities and the likely adversities to human health expected with the increase of heat waves (FERON *et al*., 2019), this research aimed to analyze the effect of climate change on the thermal comfort condition in the urban environment. As a time frame, the analysis was based on the current climate scenario and those predicted for 2050 and 2080, considering the physiological limits of the

population in a city with a tropical climate based on the application of the PET index associated with the WBT.

Methodology

The methodology proposed in this research was applied in an urban area located in the city of Vitória, Espirito Santo (ES), to fit into the climatic conditions of interest in this study and to use the PET index thermal sensation ranges, calibrated and developed by Silva and Alvarez (2015).

The following steps compose the methodology: (1) setting up future weather files; (2) defining scenarios for the simulation; (3) selecting the urban thermal comfort index; and (4) defining the human health risk assessment parameter. Figure 1 illustrates the methodological process carried out in the research.

Figure 1 – Methodological Process

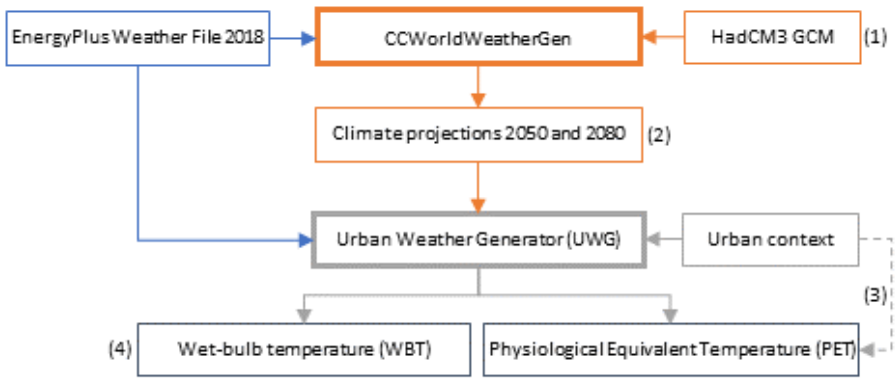

Source: the authors.

Preparing future weather files

The weather file of the city of Vitória (ES) was obtained on the Building Energy Efficiency Laboratory (LABEEE) website at the Federal University of Santa Catarina (UFSC), available for free. The file in the Energy-Plus Weather (EPW) file format, commonly used in thermal and energy simulations, includes meteorological data from the National Institute of Meteorology (INMET) measured from 2000 to 2010. Representing the current data, the weather file used in the study refers to 2018, including cloudiness data corrections (LABEEE, 2019).

There are different tools for converting a current weather file into future projections, and in this study, we chose to select a consolidated tool to use in climate simulation and analysis research, such as thermal comfort assessment in an urban community performed by Fahmi *et al.* (2017). Thus, the transformation process was carried out with the Climate Change World Weather File Generator for World-Wide Weather Data 1.9 software (CCWorldWeatherGen). The tool has free access and allows creating EPW weather files for any location in the world, considering three different time-slices: 2020, 2050 and 2080 (JENTSCH *et al.*, 2013).

The interface contains summarised data from the Hadley Centre Coupled Model version 3 (HadCM3) climate model, used in the Third and Fourth Report of the Intergovernmental Panel on Climate Change (IPCC). The A2 emission scenario was chosen to be coupled to the model, as it was heterogeneously characterised by

continuous population growth as well a slow and fragile economy (IPCC, 2007). Thus, climate projections were obtained for the city of Vitória for 2050 and 2080.

Defining simulation scenarios

In order to adapt the weather file, normally measured in the open field, to the urban context, a second procedure was carried out to convert the "rural EPW" (from 2018, 2050 and 2080) into the "urban EPW". For this purpose, it was adopted a computational tool, Grasshopper, together with a urban design plug-in called Dragonfly, through its Urban Weather Generator (UWG) component, in which the hourly values of temperature and air humidity of an urban canyon can be calculated from the climatic data measured in a meteorological station located in a rural area close to the study site (BUENO *et al*., 2013).

Other authors also adopted the tool to produce urban weather files, such as: Lima, Scalco and Lamberts (2019) for the city of Maceió, Brazil; and Evola *et al*. (2016) in Catania, southern Italy. The urban design study developed by Nakano *et al*. (2015), in which the analysis of the effects of the Urban Heat Island (UHI) was associated with global warming, relying on the methodology supported in this research.

To incorporate the effect of the ICU on the UWG, parameters were defined referring to a predetermined urban area. The city of Vitória, capital of Espírito Santo, was chosen as a case study, located in the coastal region of Southeast Brazil (MUNICÍPIO, 2020). According to the Köppen classification, the climate of Vitória can be described as Aw Tropical wet and dry, with an Am transition area (CORREA, 2014). The Aw climate has a rainy season in summer, a dry season in winter, an average temperature of the coldest month above 18°C and annual rainfall above 750 mm (EMBRAPA, 2020).

An urban portion was selected representing densely populated areas of a predominantly mixed use, with the presence of vertical buildings close to high-flow roads and the capital's financial center (Figure 2). This choice was due to the representativeness of the place both in relation to the city itself and also because it characterizes an urban typology that is quite common in Brazilian cities. Once the volumetry was modeled, the external materiality had to be builded to make it easier to calculate the weighted average of constructive information and heat exchanges analyses in the external area.

Territorial sampling comprises 26m high buildings (on average), which occupy 27% of the total area. They have a variety of uses, which are 56% residential, 41% offices and 0.03% institutions. Regarding the envelopes, the buildings have 30% to 50% of glazed facade area with glazing of 0.16 to 0.44 solar heat gain coefficient. Regarding the albedo of the surfaces, the walls present values between 0.3 and 0.9 and the coverage 0.2. Having approximately 15% of permeable area, there is an albedo of 0.25 referring to vegetation, in which the rest of the area is paved with mostly asphalt, whose albedo is equivalent to 0.1, highlighting also that the traffic is a characteristic pattern of typical mixed-use urban areas.

The climate scenarios presented in Table 1 were delimited. In order to evaluate the effect of the heat island for the selected urban area, it was decided to maintain the 2018 rural EPW for the simulation of the current condition.

Figure 2 - In (a), the selected urban clipping and in (b), the geometric model

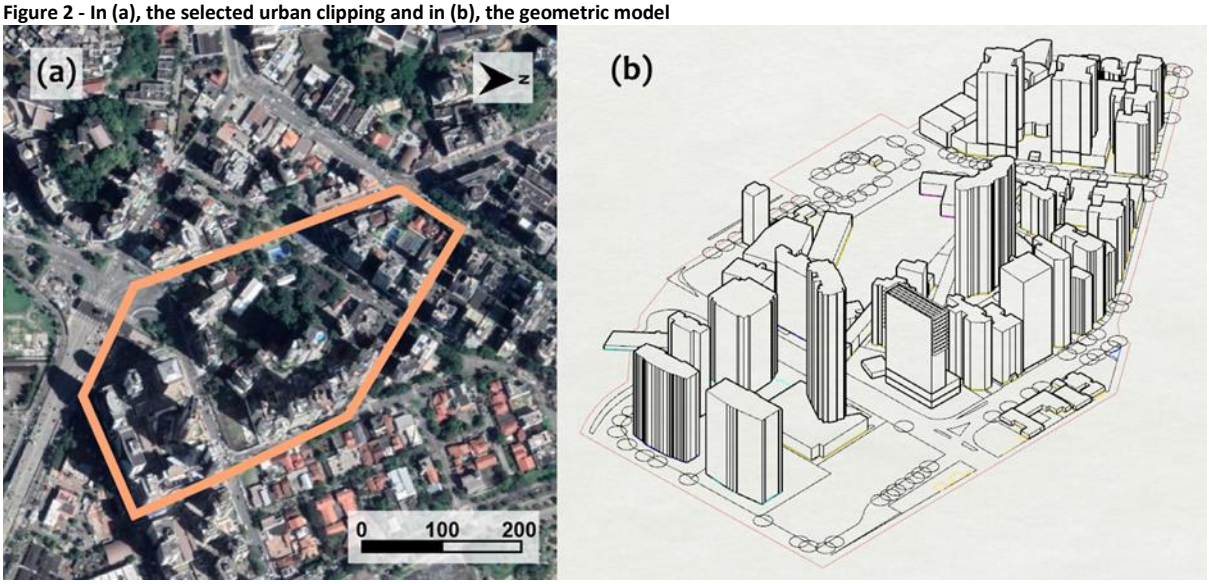

Source: the authors, adapted from Google (2019).

Table 1 - Scenarios for external thermal comfort analysis

Scenario	Description
C1	Rural weather file (rural EPW)
C2	Urban weather file (urban EPW 1)
C3	Urban Weather file with future projection for 2050 (urban EPW 2)
C4	Urban Weather file with future projection for 2080 (urban EPW 3)

Source: the authors.

Selecting the urban thermal comfort index

Ladybug tools makes enable developing an integral analysis on the same interface. Several studies employed this resource to assess the external comfort, such as Ottone *et al*. (2019), Natanian *et al*. (2020) and De Luca, Naboni and Lobaccaro (2021), who coupled the urban climate changes created by the UWG in the Grasshopper process.

As in Lucarelli, Carlo and Martinez (2020), the comfort index handled in the selected interface (Grasshopper) was PET index, based on the air temperature that allows the thermal balance of the human body under activity and heat flow conditions (COCCOLO *et al*., 2016). Therefore, the PET index was the most indicated for treating human body conditions in a physiologically relevant way (RAYMOND; MATTHEWS; HORTON, 2020).

To calculate the PET index in Grasshopper, data were applied using dry-bulb temperature (DBT) data on relative humidity, wind speed, mean radiant temperature, solar radiation analysis and body characteristics. The first three pieces of data were collected directly from the weather file, while the mean radiant temperature was calculated based on the interaction between the simulated surfaces surrounding and the DBT. Solar radiation analysis was observed by solar path and shading data, and human characteristics were standardized as a 35-year-old male, 1.75m tall and weighing 75kg; standing body position; metabolic rate of 2.32; and activities lasting 480 minutes (FRANKENFIELD, ROTH-YOUSEY, COMPHER, 2005).

Lin and Matzarakis (2008) carried out a study in a hot and humid climate, finding the neutral range between 26 and 30°C for Taiwan. There are some calibration studies in the Brazilian context, such as the one by Monteiro and Alucci (2006) for the city of São Paulo (SP); Lucchese *et al*. (2016) for Campo Grande (MS); and Kruger *et al*. (2018) for the city of Curitiba (PR). For the present study, the thermal sensation ranges defined in the PET index calibration for Vitória (ES), carried out by Silva and Alvarez (2015), were adopted, as shown in Table 2.

Table 2 - Thermal sensation and thermal stress level for the PET index for the city of Vitória

PET (°C)	Thermal stress level
18°C < PET ≤ 20°C	Cold
20°C < PET ≤ 22°C	Slightly cold
22°C < PET ≤ 30°C	Neutral (comfortable)
30°C < PET ≤ 34°C	Slightly hot
34°C < PET ≤ 46°C	Hot
> 46°C	Very hot

Source: the authors, adapted from Silva and Alvarez (2015).

Defining the human health risk assessment parameter

To assess the human health risk assessment, the WBT variable was defined as an analysis parameter. It is known that the human body has difficulties in cooling its internal temperature when found in a humid environment that prevents evapotranspiration from the skin surface and, thus, performs the body's thermoregulation. In a critical situation, when the environment is at a WBT of 35°C, thermoregulation is prevented naturally, resulting in a risk to the integrity and health of the human body, and this value is considered as the physiological limit to human survival. (ASHRAE, 2017; RAYMOND, MATTHEWS, HORTON, 2020; THORSSON *et al*., 2020).

In a recent climatological study, Raymond, Matthews and Horton (2020) emphasize that certain climatic conditions, usually when the WBT is above 26°C, are more dangerous for people with more fragile health conditions such as the elderly. They also point out that mortality episodes caused by WBT values lower than 35°C were verified in regions of Europe in 2003 and in Russia in 2010, which, although severe, both recorded WBT values not exceeding 28°C.

Based on the method proposed by Sullivan and Sanders (1974), the WBT calculation was performed taking into account both the humidity and the DBT and the barometric pressure by the height of the climatic data measurement station. Thus, the number of annual hours in which the WBT is above the ranges considered at risk (26°C and 35°C) was evaluated.

Results and Discussion

Urban heat island phenomenon

The comparison between the data obtained in the simulation of the C1 scenario (Table 1) and in the C2 scenario (Table 1) allowed to measure the influence of urban parameters such as vegetation, paving and built volume in the urban environment. As observed in Figure 3, there was a tendency for an increase in external temperature in the urban area when compared to the rural environment. When analysing the monthly average temperature in both scenarios, a difference of up to 1.91°C was observed in the values obtained for the same month.

The DBT annual average obtained in the C1 scenario was 24.35°C, while in the C2 scenario it was 25.56°C, that is, a difference of 1.16°C, thus demonstrating the effective influence of humidity on the temperature of the environment. Regarding seasonal temperature variations, both scenarios presented August as the lowest monthly average, and in the first scenario the value obtained was lower than the second, respectively, 21.68°C and 23.08°C.

Figure 3 - Monthly temperature average in scenarios C1 and C2

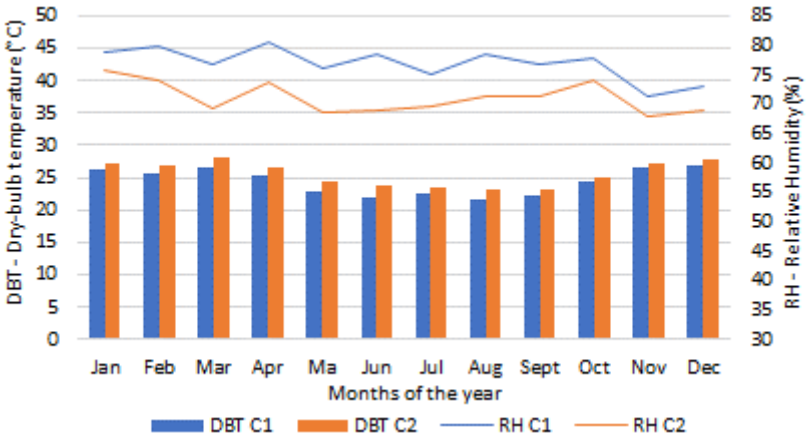

Source: the authors.

Unlike the result observed in the winter, there was a divergence in the hottest month of each scenario for the summer season. In the first scenario, December presented the highest monthly average (26.86°C), while in the second, this phenomenon occurred in March (28.17°C). This difference in average between the traditionally warmer months can hint the severity of weather conditions in urban areas.

Regarding air humidity, all months in the urban scenario had a lower value than in the rural scenario. The most significant difference in the monthly average was observed in June, in which a value of 78.47% was obtained in the C1 scenario and 68.82% in the C2 scenario. April had the highest percentage of humidity in C1 (80.55%), while in C2, November had the lowest rate (67.95%). Thus, throughout the year, there may be a reduction of 12.60% in humidity concomitant with an increase of 3.78°C in the temperature.

These results show the occurrence of the urban heat island, according to the concept defended by Oke *et al.* (2017). It should be noted that the addition of the urban form element modeling in the C2 scenario resulted in the occurrence of phenomena that were not considered in the first scenario simulation, such as the shading effect of the built volume and the obstruction, absorption and reflection of solar radiation by the building surfaces.

Climatic conditions of urban scenarios

Figure 4 presents the monthly average of DBT obtained in the simulated scenarios, in which a warming trend is observed over the years. Thus, a gradual increase in the annual average temperature of 1.69°C and 1.49°C, respectively, was observed in the selected future years. To effectively verify this global warming trend, it would be necessary to carry out a modeling of reliable climate scenarios for a later period.

In June, the highest temperature increase was observed with the replacement of the scenarios, with an increase of 2.18°C and 1.73°C in 2050 (C3) and 2080 (C4), respectively. All urban scenarios presented March as the highest monthly average temperature. In scenarios C2 and C3, the lowest monthly average was obtained in August, while in C4, this value was obtained in September.

When comparing the results obtained in the simulation with the data monitored by INMET, it can be observed that the months that presented the highest and lowest averages coincided with the typical summer and winter periods observed in the climatic history of the city. It is noteworthy that the analysis method used by INMET (2020) is

based on meteorological data for an indicated period of thirty consecutive years (from 1931 to 1960, 1961 to 1990 and 1991 to 2010), subject to data availability.

Figure 4 - Monthly temperature and humidity average for urban scenarios C2, C3 and C4

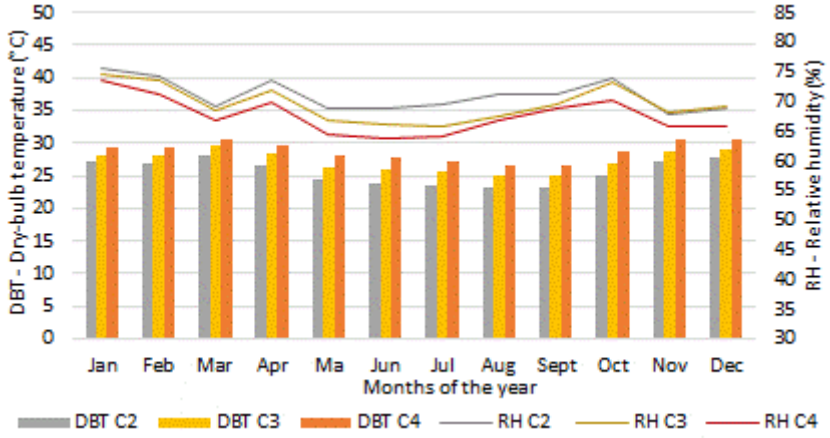

Source: the authors.

As seen in Figure 5, all simulated scenarios illustrated higher averages than the values obtained in the periods analyzed by INMET (2020). Although these values correspond to the typical weather pattern of the local summer and winter seasons, no closeness was observed between the hottest and coldest months observed in the survey and in the monitored data.

Figure 5 - Monthly temperature data measured by INMET and simulated for scenarios C2, C3 and C4

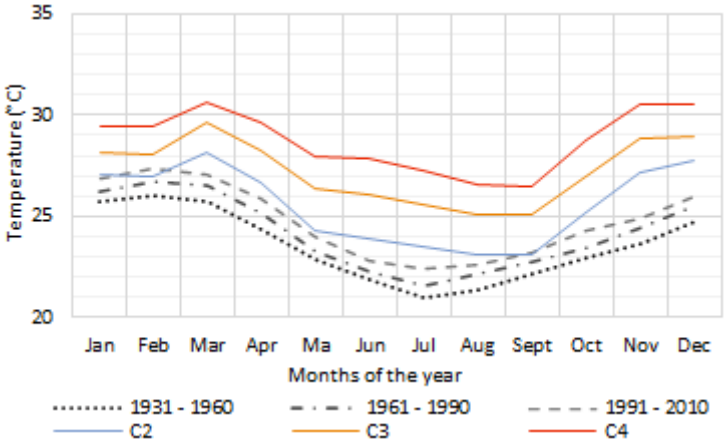

Source: the authors, adapted from INMET (2020).

In the INMET data (2020), the highest monthly averages of temperature occurred in February, while in the simulated scenarios the highest temperatures were observed in March and December. April had the highest thermal increase over the monitored periods (1.6°C), while in the survey, this increase was observed in June (3.91°C).

It should be noted that the future weather file submitted to the climate changes predicted in the A2 emission scenario of the fourth IPCC report contributed significantly to the increase in external temperature, whose result confirm the climate projections indicated by the Intergovernmental Panel on Climate Change (IPCC, 2007). Studies produced in Brazil obtained similar results, such as those by Guarda *et al*. (2020) in the city of Cuiabá; and Triana, Lamberts and Sassi (2018) for the cities of Salvador and São Paulo.

Regarding air humidity, there was a tendency to reduce the annual average with the evolution of urban scenarios. Thus, a decrease of 1.57% was observed when comparing C2 and C3 and 2.21% between C3 and C4. January presented the highest monthly average in the three scenarios, with a value of 75.65%, 74.73% and 73.71% respectively.

As with the temperature in the summer, there was no connection regarding the months with the lowest monthly averages of humidity. In scenario C2, this value was obtained in November (67.95%), while in C3, the lowest value was observed in July (65.92%). In turn, in the C4 scenario, the lowest monthly average was observed in June (63.85%).

Urban thermal comfort

Considering that in tropical regions with a hot-humid climate, excess heat corresponds to one of the main climatic aspects to be controlled for thermal balance in external environments (ROMERO, 2000), associated with global warming trend observed in the data simulated in the research, we chose to focus on the climatic analysis for the summer period, whose time frame encompasses December to March.

Figure 6 shows the PET index isograms for the aforementioned period. The coloring is associated with the thermal sensation levels defined in the study by Silva and Alvarez (2015), who propose the calibration of values for the city of Vitória. The dark blue color indicates the times when there is a cold thermal sensation, which will minimize to comfortable levels, represented by the lighter tones. The transition to yellow synthesizes the values corresponding to the gradual increase in heat, reaching levels of heat stress in red.

In C2, from midnight to 7 am, blue prevails, with the highest proportions of slightly cold and cold thermal sensation, especially in January. From 9 am, the appearance of yellow tones can be observed, which intensifies in the morning until reaching the peak temperature (red) close to 1 pm. In general, it was observed that the thermal gain started in the morning lasts until 17:00 and the highest temperatures are concentrated from 11:00 to 15:00.

In the late afternoon, there is an inverse effect of color fading, at a slow pace due to the urban heat island, in which the temperature remains high during the night. In this period of the day, the extension of yellow can occur until midnight, exemplified by the days on January 21 and February 11, and in March, the warm tones last longer (days and hours).

For the C3 scenario, the transition from blue to the predominance of yellow is observed, demonstrating that the hot thermal sensation can last for up to 24 hours. In contrast to the other months, January continues to show a uniform distribution of slightly cold hours in the morning and at night, as well as a concentration during most of the day, between February 12th and 15th. Unlike these months, which still have a great predominance of blue in medium and dark tones, December has a gradual transposition where March has practically no hours in this pattern.

In C3, temperatures with less variability are observed when compared to the C2 scenario. In December and March, a thermal gain was observed starting at 8 am and lasting until 6 pm. In January and February, there was a thermal gain from 9 am that remained until 6 pm. In general, the highest temperatures are concentrated in the 10 am to 4 pm range.

Figure 6 - Isograms of the PET index referring to urban scenarios (C2, C3 and C4)

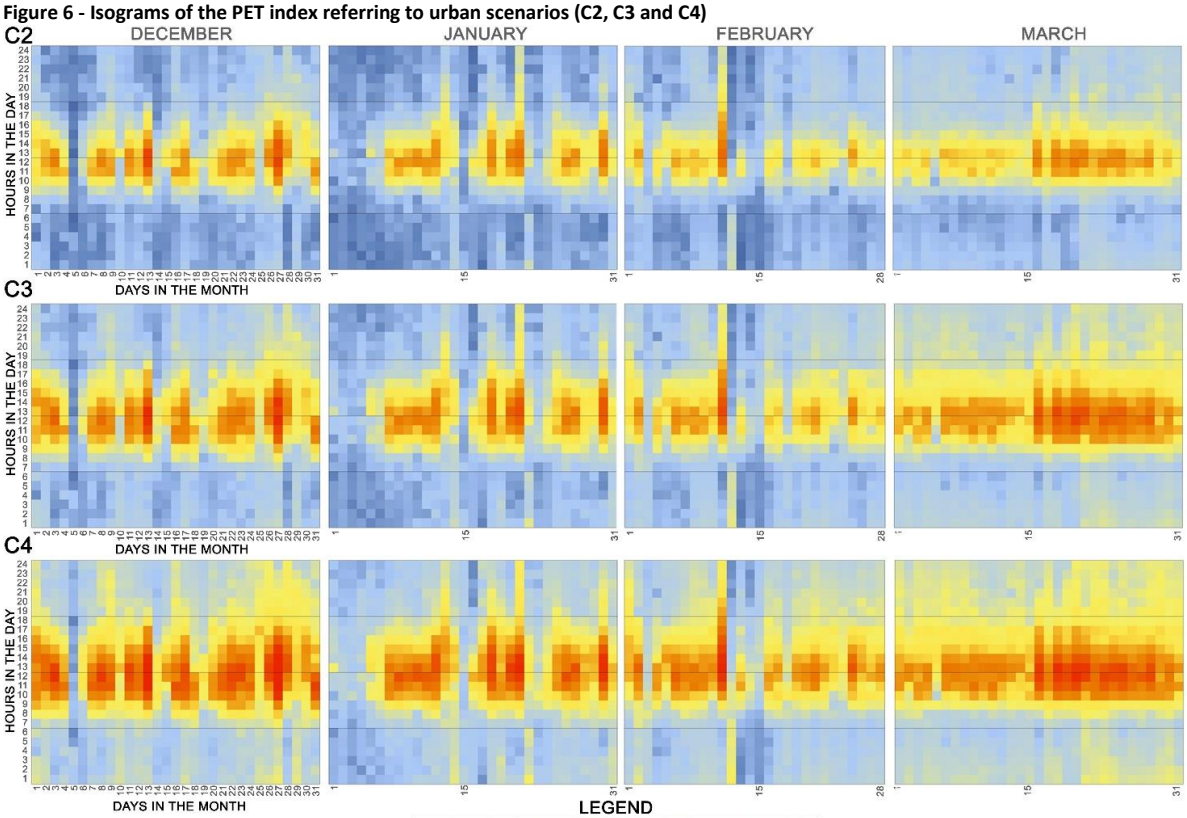

LEGEND

COLOUR	PET INDEX	THERMAL SENSATION RANGE
Dark red	> 46°C	Very hot
Light red	46°C - 43°C	Hot
Dark orange	43°C - 39°C	Hot
Light orange	39°C - 36°C	Hot
Dark yellow	36°C - 32°C	Hot
Light yellow	32°C - 29°C	Slightly hot
Light blue	29°C - 25°C	Neutral
Medium blue	25°C - 22°C	Neutral
Dark blue	22°C - 18°C	Slightly cold and cold

Source: the authors, based on Silva and Alvarez (2015).

In the last C4 scenario, the warming process is more evident, especially in March and December. It can be seen that blue tends to stand out in a light tone at the same time that the yellow expands through the isograms. The color transformation takes place especially in January and March, and has a substantial reduction in the cold sensation in January, which on the contrary, an accelerated increase in the warm tones is observed in March.

In January, there may be a level reduction of up to 28.36% associated with cold until 2080, while in March, for the same period, the trend is for an increase of 27.82% in hot temperatures. The concentration of warm tones in the daytime can be seen, which expands throughout the scenarios and can reverse the predominance with cold tones. In general, a thermal gain is observed from 8 am that lasts until 8 pm. In C4, the highest temperatures are concentrated in the period from 9 am to 4 pm, indicating the expansion of the hourly interval with high temperatures throughout the day, at the same time with the reduction of colder intervals. This concentration of very hot temperatures can lead to thermal stress, so that the user cannot withstand the heat for consecutive hours.

The isograms indicate an increase of up to 3 hours in the period referring to the slightly warm and hot thermal sensation in future scenarios. Orange and red appear concentrated in the afternoon at C2 while, in later years, they expand to other times, causing an increase of up to 4 hours in the period of exposure to temperatures above

39°C PET. In addition, the reduction of the night cooling process and the intensification of the hot temperature, represented by the red hue, is evident.

Despite the phenomenon previously mentioned, the temperature oscillations between the levels of thermal sensation indicate a percentage of comfort hours above 50% in all scenarios due to the reduction of the slightly cold sensation (mainly at the beginning and end of the day), in which January and February are the most benefited in this process. As they are the hottest months, March and December had the lowest comfort rates of the season. This modification of the monthly temperatures of the PET can be seen in Figure 7, by comparing the number of hours corresponding to each range of thermal sensation determined by the index.

Figure 7 - Number of hours for each PET thermal range adapted to Vitória for scenarios C2, C3 and C4

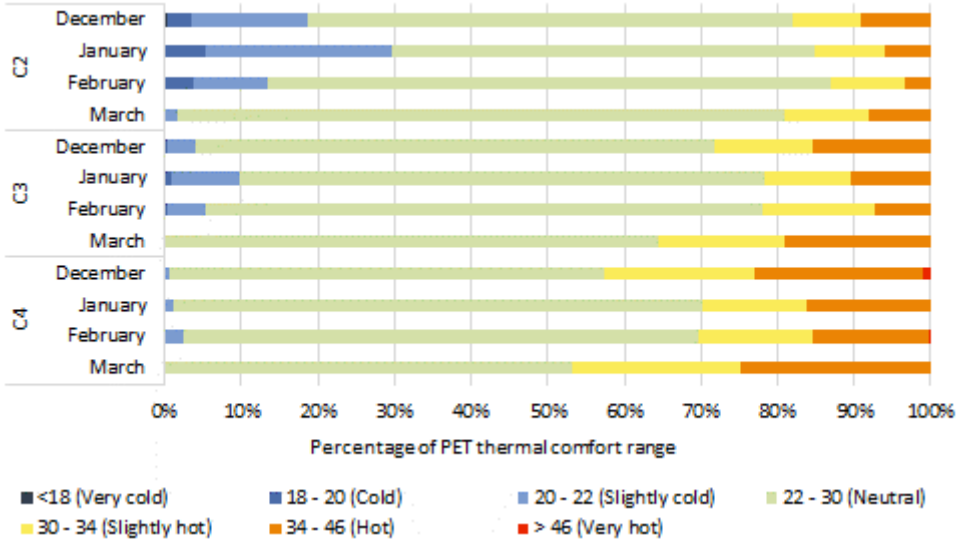

Source: the authors.

Analyzing the thermal trend of the PET index, December presented a very cold sensation (<18°C) only in the C2 scenario, in about 0.40% of hours. On the other hand, this month, the highest percentage of hours at the hot level (34-46°C) was found, approximately 9.27%, which intensified in C3 and C4, resulting in 15.25% and 22.17%, respectively. In C4, 0.94% of hours were observed for the very hot level and 0.13% of hours for the cold level, highlighting a large thermal amplitude in that month.

In January, the highest amount of hours was observed in the slightly cold and cold levels in C2. However, with the gradual reduction of these two thermal sensation ranges in future years, it was configured as the best panorama of thermal comfort, reaching 68.95% in C4. In turn, February showed the smallest reduction in comfort hours in the scenarios, from 73.66% in C2 to 67.11% in C4. Similar to December, February recorded monthly hours at a very hot level (extreme stress) above 46°C.

March stands out for not having a PET temperature between 18°C and 20°C and only 1.61% of hours with a slightly cold thermal sensation in C2, as well as the greatest reduction in comfort hours between C2 and C4 (26.21 %). Most of the hours in this month have temperatures at slightly hot and hot levels when compared to the other months of the season, in which an increase of up to 11.15% and 16.67%, respectively, was observed.

To understand the microclimatic dynamics, the daily PET temperature profile of the hottest day in March was prepared (Figure 8). It can be seen that the minimum value (20.57°C) occurs at 6 am. From that time onwards, a thermal gain was observed that

reached between 35°C and 45°C, from 10 am to 4 pm. At night, there is a slow attenuation of the external temperature.

Figure 8 - PET temperature in the hourly profile of the hottest day (16) of March in scenarios C2, C3 and C4

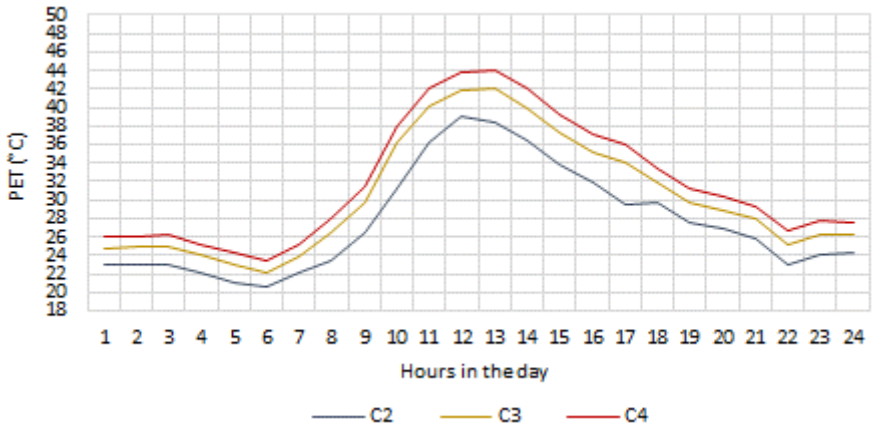

Source: the authors.

Another important condition is the temperature difference between scenarios, where from C2 to C3 there is an increase of 3°C at the moment of the thermal peak, and for C4 this increase was lower, contributing to a maximum temperature of 43.98°C. It is noteworthy that the daily thermal amplitude in C2 (2018) is 18.46°C, while in the other scenarios the amplitude is even greater with C3 (2050) presenting 20°C and C4 (2080), 20.65°C, however, there was not a large variation in amplitude between them, which corroborates the hourly temperature data for hotter days.

However, in Figure 9, it can be seen that there is no constant temperature during the summer season, in which times of extreme thermal peaks were presented, such as the minimum value of 20.48°C in January in the C3 scenario, and especially in December in C4, in which the temperature reached a maximum value of 49.39°C at 12:00. This same day can reach the margin of 45.83% of the day with temperatures above 34°C (hot level), with 11.67% in extreme heat levels.

Figure 9 - Hourly PET temperature in the summer, on the left for scenario C3 and on the right for scenario C4

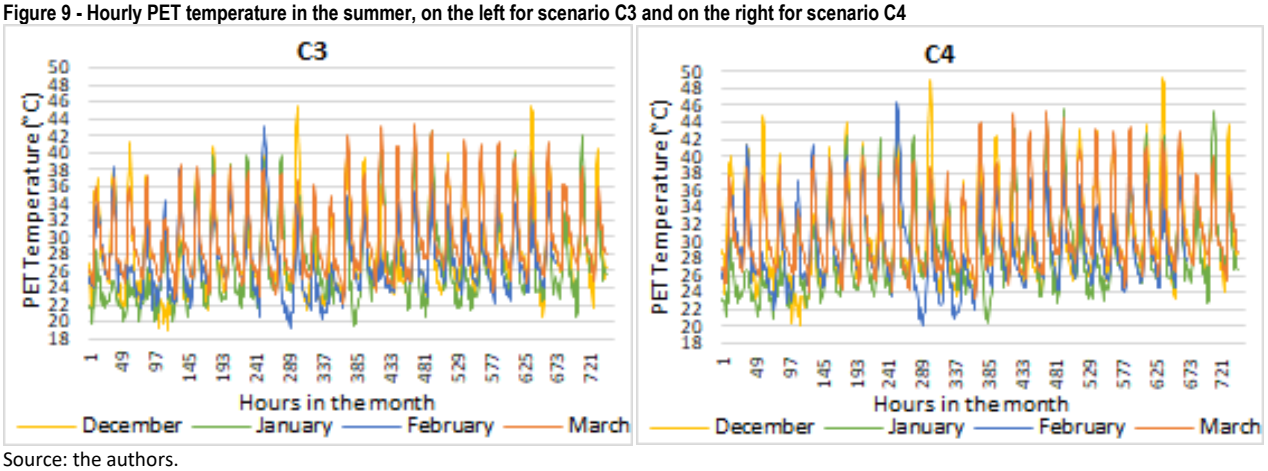

Source: the authors.

Although the frequency of very hot temperatures was lower than the hot level, the predominance of the latter can already bring about feelings of discomfort and malaise in most months. In turn, the increase in the average temperature associated with the occurrence of warmer levels for more hours in the year, can culminate in a greater frequency of extreme events, with temperature records and/or heat waves.

Given this scenario, some individual forms of progressive prevention can be adopted, according to the level of heat, respectively, from the lowest to the highest risk, such as: i) increasing hydration and seeking shade; ii) reducing prolonged exposure from 10 am to 4 pm, as well as staying or exercising in a cool place; iii) cancelling outdoor activities during the hours when it is hot; and iv) staying in a cool place even at night (NOAA, 2021).

In a comprehensive and effective way, through the combined analysis of future climate projections and urban thermal comfort indices, the likely future effects on human health can be assessed and, thus, direct actions - public or private - for mitigation. of undesirable consequences.

Human health risk

As previously mentioned, heat extremes can occur due to high temperature or the combination of humidity and heat, which makes the outdoor condition more unpleasant (CLIMATE, 2016). The correlation between the WBT data and the PET thermal sensation range makes it possible to assess the physiological risk using human thermoregulation as a parameter, associated with the PET thermal sensation ranges.

At first, the number of annual hours in which the WBT is above 26°C was observed, in which a percentage of 2.68% was obtained for the C3 (2050) scenario and reaching considerable values in C4 (2080), with 14.32%. Thus, it can be observed that both DBT and WBT intensify throughout the scenarios. This increase occurs in different proportions, accentuating the difference between temperatures up to C4 and, consequently, indicating the low relative air humidity.

A WBT value equal to or greater than the physiological limit of 36°C was not found, however, it is noteworthy that values of 30°C were observed (considered high risk) in all scenarios. The number of hours under these conditions was reduced by about 5h in 2018 and 2h in 2050 and 2080, predominantly in the morning and in May to September. The occurrence of this phenomenon in the aforementioned period can be justified by the increase in DBT in high proportions in both scenarios, combined with the low reduction in relative humidity. It is important to highlight that May to September were the ones that warmed the most in future years, obtaining increases above the values observed for other seasons.

For the same day, the results achieved in this study showed that, at times, the PET temperature found in the climate projections corresponds to the ranges considered to be at risk for people's health. In summer, for example, the warm level PET comfort range (34°C to 46°C) coincides with a high WBT value from 3 pm to 5 pm, with the possibility of extending this range.

As seen earlier, warm PET index levels are concentrated mainly in the afternoon, while high WBT tend to extend into the night period, a condition that is noticeable in the C3 and C4 scenarios. To exemplify this, February in C4 presented high values of WBT until 22h, in which a compatibility of temperatures was observed until 20h.

For the same C4 scenario, December and January were the ones with the highest number of hours with risks arising from the WBT, in which more than 50% of the day showed values above 26°C. Among these hours, the first month of the season showed a special consideration, since in the period from 9 am to 6 pm there may be an association between the hot to very hot comfort range and the health risk level depending on the values found for the WBT (Figure 10).

Figure 10 - Hourly PET and wet-bulb temperature on the hottest day (December 27) for scenarios C3 and C4

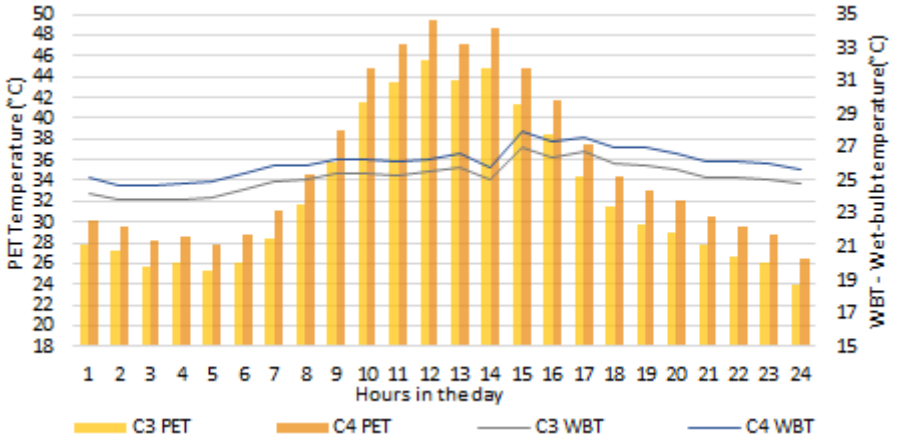

Source: the authors.

At 1 pm, atypical behavior can be observed both in PET index and WBT, with a reduction in the first and a brief increase in the second. This can be explained by the humidity data reaching higher values at this time, contributing to the increase in the water vapor content in the air and heat attenuation.

On the other hand, WBT reaches the lowest value at 2 pm, concomitant with the second highest PET temperature. This phenomenon is related to the low relative humidity index associated with the high DBT observed at the time. It is known that relative humidity varies as a function of day temperature changes, determining the potential capacity of the air to contain a certain amount of water vapor (ROMERO, 2000). The environment condition of low saturation and high DBT helps to widen the difference between the values obtained by the latter experiment and the WBT.

Considering the aforementioned, the need for strategies is clear, both to mitigate the heat island effect along with to control air humidity, which are fundamental to establish thermal comfort. The balance of these thermal variables, aiming at increasing the comfort conditions in the city, can encourage the permanence of users in external environments, especially in a context of increasing life expectancy in urban communities, in line with the increase in the percentage of elderly people living in cities. Some improvements in urban thermal comfort levels can be encouraged, such as the expansion of urban afforestation and increasing shading elements, as well as regulating cities and its growth, particularly when considering the need to leave the path of prevailing winds clear.

Conclusion

Adopting a holistic method regarding the prediction of thermal stress, relating physiological aspects to climatological variables, offers a relevant insight to human thermal comfort analysis in urban areas. Thus, this article has the objective to present a concise result that aims to break down the effect of climate change on the thermal comfort condition and on the physiological limit of the population, in a city with a tropical climate, using the PET index together with WBT data.

The innovations required to carry out this study were focused around an integrated methodology that combined thermal, urban and physiological components. Thus the effect of the heat island and climate change on urban thermal comfort in predictive scenarios was assessed by comparing climatic variables and computing hourly thermal sensation data, using the same tool. From another perspective, given the evaluated scale, it was found that the microclimatic analysis is relevant in the investigation of

thermal comfort at a pedestrian scale, such as the representation of PET temperatures by bioclimatic mapping and the fluid dynamics of the territorial sampling.

By running computer simulations, a heating trend was identified with the evolution of the scenarios and, consequently, the reduction of daily thermal comfort hours. The thermal gain resulting from the climate projections predicted for 2050 and 2080, caused a reduction in the cooling process, mainly at night. These results showed evidence of the occurrence of the urban heat island phenomenon, restating the influence of the built environment elements on the local climate dynamics. Thus, an unquestionable influence of vegetation on local humidity is highlighted, which was not discussed in depth in the analysis of this research.

In addition to the increase in the hourly interval at warm levels, the PET temperature data indicated the presence of heat stress in the summer until 2080, mainly in the daytime period. The comparison with the WBT enabled us to establish that between 3 pm and 5 pm, with the possibility of an hourly extension, people may be vulnerable to both situations of discomfort, which means, high temperatures and thermal sensation of heat due to relative humidity. In addition, the human health risk worsened from the increase of annual hours in which the WBT is in the range of 26°C to 30°C in the evolution of scenarios.

It is noteworthy that the human physical characteristics standardized when calculating the PET index describe an adult in a normal thermal state. Therefore, applying the same climatic conditions over people from vulnerable groups can cause more severe risks, depending on the exposure time, such as dehydration and heat stroke. In order to mitigate the future consequences on people's health, it is necessary to adopt urgent measures, by establishing lasting public policies and urban regulation instruments, including the effective participation of the private sector in this process, also responsible for the consequences inherent to the climate changes.

Acknolegments

This study was financed in part by the Coordenação de Aperfeiçoamento de Pessoal de Nível Superior – Brasil (CAPES) – BOLSAS DS/CAPES MESTRADO Code: 30001013030P1. The authors thank the *Laboratório de Planejamento e Projetos* of the Federal University of Espírito Santo (LPP/UFES) for all the technical support required to push the present research further.

References

ASHRAE. AMERICAN SOCIETY OF HEATING, REFRIGERATING AND AIR-CONDITIONING ENGINEERS. **The ASHRAE Handbook of Fundamentals**. Peachtree Corners: American Society of Heating, 2017. 1013 p.

BATHIANY, S.; DAKOS, V.; SCHEFFER, M.; LENTON, T. M. Climate models predict increasing temperature variability in poor countries. **Science Advances**, v. 4, n. 5, May 2018. DOI: https://doi.org/10.1126/sciadv.aar5809.

BUENO, B.; NORFORD, L.; HIDALGO, J.; PIGEON, G. The urban weather generator. **Journal of Building Performance Simulation**, v. 6, n. 4, p. 269-281. 2013. DOI: https://doi.org/10.1080/19401493.2012.718797 .

CLIMATE Change and Extreme Heat: What You Can Do to Prepare. Washington, DC: Environmental Protection Agency (EPA); Centre's for Disease Control and Prevention (CDC). Oct. 2016. 20 p. Disponível em: https://www.cdc.gov/climateandhealth/pubs/extreme-heat-guidebook.pdf. Acesso em: 21 maio 2021.

COCCOLO, S.; KÄMPF, J.; SCARTEZZINI, J. L.; PEARLMUTTER, D. Outdoor human comfort and thermal stress: A comprehensive review on models and standards. **Urban Climate**, v. 18, p. 33-57, Dec. 2016. DOI: https://doi.org/10.1016/j.uclim.2016.08.004.

CORREA, W. S. C. **Campo térmico e higrométrico da Regional Praia do Canto no município de Vitória (ES)**. 2014. 165 p. Dissertação (Mestrado em Geografia) – Centro de Ciências Humanas e Naturais. Universidade Federal do Espírito Santo, Vitória, 2014. Disponível em: http://repositorio.ufes.br/handle/10/1193. Acesso em: 15 mar. 2022.

DE LUCA, F.; NABONI, E.; LOBACCARO, G. Tall buildings cluster form rationalization in a Nordic climate by factoring in indoor-outdoor comfort and energy. **Energy & Buildings**, v. 238, p. 110831, May 2021. DOI: https://doi.org/10.1016/j.enbuild.2021.110831.

EMBRAPA. EMPRESA BRASILEIRA DE PESQUISA AGROPECUÁRIA. **Clima.** Brasília: Embrapa, 2020 Disponível em: https://www.cnpf.embrapa.br/pesquisa/efb/clima.htm. Acesso em: 13 nov. 2020.

EVOLA, G.; COSTANZO, V.; MAGRÌ, C.; MARGANI, G.; MARLETTA, L.; NABONI, E. A novel comprehensive workflow for modelling outdoor thermal comfort and energy demand in urban canyons: Results and critical issues. **Energy & Buildings**, v. 216, p. 109946, June 2020. DOI: https://doi.org/10.1016/j.enbuild.2020.109946.

FAHMY, M.; EL-HADY, H.; MAHDY, M.; ABDELALIM, M. F. On the green adaptation of urban developments in Egypt; predicting community future energy efficiency using coupled outdoor-indoor simulations. **Energy and Buildings**, v. 153, p. 241-261, Oct. 2017. DOI: https://dx.doi.org/10.1016/j.enbuild.2017.08.008.

FERON, S.; CORDERO, R. R.; DAMIANI, A.; LLANILLO, P. J.; JORQUERA, J.; SEPULVEDA, E.; ASENCIO, D.; LAROZE, D.; LABBE, F.; CARRASCO, J.; TORRES, G. Observations and Projections of Heat Waves in South America**. Scientific Reports**, v. 9, 8173, June 2019. DOI: https://doi.org/10.1038/s41598-019-44614-4.

FRANKENFIELD, D.; ROTH-YOUSEY, L.; COMPHER, C. Comparison of Predictive Equations for Resting Metabolic Rate in Healthy Nonobese and Obese Adults: A Systematic Review. **Journal of the American Dietetic Association**, v. 105, n. 5, p. 775–789, May 2005. DOI: https://doi.org/10.1016/j.jada.2005.02.005.

GOOGLE. **GOOGLE EARTH**: Versão Pro. Mountain View: GOOGLE, 2019. Disponível em: https://www.google.com/intl/pt-BR/earth/versions/#earth-pro. Acesso em: 20 nov. 2019.

GUARDA, E. L. A.; DOMINGOS, R. M. A.; JORGE, S. H. M.; DURANTE, L. C.; SANCHES, J. C. M. LEÃO, M.; CALLEJAS, I. J. A. The influence of climate change on renewable energy systems designed to achieve zero energy buildings in the present: A case study in the Brazilian Savannah. **Sustainable Cities and Society**, v. 52, p. 101843, Jan. 2020. DOI: https://doi.org/10.1016/j.scs.2019.101843.

HÖPPE, P. The physiological equivalent temperature - a universal index for the biometeorological assessment of the thermal environment. **International Journal of Biometeorology,** v. 43, p. 71–75, Oct. 1999. DOI: https://doi.org/10.1007/s004840050118.

INMET. INSTITUTO NACIONAL DE METEOROLOGIA. **Clima**. Normais climatológicas. Gráficos. Brasília: INMET, 2020. Disponível em: https://clima.inmet.gov.br/GraficosClimatologicos/DF/83377. Acesso em: 13 nov. 2020.

IPCC. INTERGOVERNMENTAL PANEL ON CLIMATE CHANGE. **Climate Change 2007:** The Physical Science Basis. Contribution of Working Group I to the Fourth Assessment. Report of the Intergovernmental Panel on Climate Change. Brussels: IPCC, 2007. 996 p. Disponível em: https://www.ipcc.ch/site/assets/uploads/2018/05/ar4_wg1_full_report-1.pdf. Acesso em: 08 nov. 2019.

JENTSCH, M. F.; JAMES, P. A. B.; BOURIKAS, L.; BAHAJ, A. S. Transforming existing weather data for worldwide locations to enable energy and building performance simulation under future climates. **Renewable Energy**, v. 55, p. 514-524, July 2013. DOI: https://doi.org/10.1016/j.renene.2012.12.049.

KRÜGER, E. L.; ROSSI, F. A.; CRISTELI, P. S. SOUZA, H. A. Calibração do índice de conforto para espaços externos *Physiological Equivalent Temperature* (PET) para Curitiba. **Ambiente Construído**, v. 18, n. 3, p. 135-148, jul./set. 2018. DOI: http://dx.doi.org/10.1590/s1678-86212018000300272.

LABEEE. LABORATÓRIO DE EFICIÊNCIA ENERGÉTICA EM EDIFICAÇÕES. **Arquivos climáticos INMET 2018**. Florianópolis: UFSC, 2019. Disponível em: https://labeee.ufsc.br/downloads/arquivos-climaticos/inmet2018. Acesso em: 20 jun. 2021.

LAPOLA, D. M.; SILVA, J. M. C.; BRAGA, D. R.; CARPIGIANI, L.; OGAWA, F.; TORRES, R. R.; BARBOSA, L. C. F.; OMETTO, J. P. H. B.; JOLY, C. A. A climate-change vulnerability and adaptation assessment for Brazil's protected areas. **Conservation Biology**, v. 34, n. 2, p. 427-437, Aug. 2019. DOI: https://doi.org/10.1111/cobi.13405.

LIMA, I.; SCALCO, V.; LAMBERTS, R. Estimating the impact of urban densification on high-rise office building cooling loads in a hot and humid climate. **Energy & Buildings**, v. 182, p. 30-44, Jan. 2019. DOI: https://doi.org/10.1016/j.enbuild.2018.10.019.

LIN, T. P.; MATZARAKIS, A. Tourism climate and thermal comfort in Sun Moon Lake, Taiwan. **International Journal of Biometeorology**, v. 52, p. 281–290, Oct. 2008. DOI: https://doi.org/10.1007/s00484-007-0122-7.

LUCARELLI, C. C.; CARLO, J. C.; MARTINEZ, A. C. P. Otimização baseada em simulação para uma cobertura inspirada em origami. **PARC Pesquisa em Arquitetura e Construção**, v. 11, ago. 2020. DOI: https://doi.org/10.20396/parc.v11i0.8658250.

LUCCHESE, J. R.; MIKURI, L. P.; FREITAS, N. V. S.; ANDREASI, W. A. Application of Selected Indices on Outdoor Thermal Comfort Assessment in Midwest Brazil. **International Journal of Science and Engineering Investigations**, v. 7, n. 4, p. 291-302, 2016. Disponível em: http://www.ijee.ieefoundation.org/vol7/issue4/IJEE_03_v7n4.pdf. Acesso em: 20 jan. 2022.

MATZARAKIS, A.; MAYER, H.; IZIOMON, M. G. Applications of a universal thermal index: physiological equivalent temperature. **International Journal of Biometeorology**, v. 43, p. 76–84, Oct. 1999. DOI: https://doi.org/10.1007/s004840050119.

MAUREE, D.; NABONI, E.; COCCOLO, S.; PERERA, A. T. D.; VAHID, M. N.; SCARTEZZINI, J. L. A review of assessment methods for the urban environment and its energy sustainability to guarantee climate adaptation of future cities. **Renewable and Sustainable Energy Reviews**, v. 112, p. 733-746, Sept. 2019. DOI: https://doi.org/10.1016/j.rser.2019.06.005.

MONTEIRO, L. M.; ALUCCI, M. P. Calibration of Outdoor Thermal Comfort Models. *In*: CONFERENCE ON PASSIVE AND LOW ENERGY ARCHITECTURE, 23., Geneva, 2006. **Proceedings [...].** Geneva: PLEA, 2006.

MUNICÍPIO de Vitória: Estado do Espírito Santo. [*S. l.*], 2020. Disponível em: https://www.cidade-brasil.com.br/. Acesso em: 10 jun. 2021.

NAKANO, A.; BUENO, B.; NORFORD, L.; REINHART, C. F. Urban Weather Generator - A novel workflow for integrating urban heat island effect within urban design process. *In*: INTERNATIONAL BUILDING PERFORMANCE SIMULATION ASSOCIATION, 14., 2015. **Proceedings [...].** Hyderabad, 2015. p. 1901-1908. Disponível em: http://urbanmicroclimate.scripts.mit.edu/files/IBPSA_2015_Nakano.pdf. Acesso em: 20 mar. 2022.

NATANIAN, J.; KASTNER, P.; DOGAN, T.; AUER, T. From energy performative to livable Mediterranean cities: An annual outdoor thermal comfort and energy balance cross-climatic typological study. **Energy & Buildings**, v. 224, Oct. 2020. DOI: https://doi.org/10.1016/j.enbuild.2020.110283.

NOAA. NATIONAL OCEANIC AND ATMOSPHERIC ADMINISTRATION. **National Weather Service**: Experimental HeatRisk. 2021. Disponível em: https://www.wrh.noaa.gov/wrh/heatrisk/pdf/HeatRisk_More_Info_Web.pdf. Acesso em: 12 jan. 2022.

OKE, T. R; MILLS, G.; CHRISTEN, A.; VOOGT, J. A. **Urban Climates**. Cambridge: Cambridge University, 2017, 546 p.

OTTONE, M. F.; COCCI GRIFONI, R.; MARCHESANI, G. E.; RIERA, D. Density - intensity. Material and immaterial elements in assessing urban quality. **Journal of Technology for Architecture and Environment**, v. 17, p. 278-288.

2019. Disponível em: https://oaj.fupress.net/index.php/techne/article/view/5064/5064. Acesso em: 20 jan. 2022. Artigo em inglês e italiano.

RAYMOND, C.; MATTHEWS, T.; HORTON, R. M. The emergence of heat and humidity too severe for human tolerance. **Science Advances,** v. 6, n. 19, 2020. DOI: https://doi.org/10.1126/sciadv.aaw1838.

RIBEIRO, S. K.; SANTOS, A. S. **Mudanças Climáticas e Cidades**. Relatório Especial do Painel Brasileiro de Mudanças Climáticas. Rio de Janeiro: COPPE – UFRJ, 2016. 116p. Disponível em: http://www.pbmc.coppe.ufrj.br/documentos/Relatorio_UM_v10-2017-1.pdf. Acesso em: 20 jan. 2022.

ROMERO, M. A. B. **Princípios bioclimáticos para o desenho urbano**. São Paulo: Proeditores, 2000, 128p.

SCHÄR, Christoph. The worst heat waves to come. **Nature Climate Change**, v. 6, p. 128-129. 2016. DOI: https://doi.org/10.1038/nclimate2864.

SHERWOOD, S. C.; HUBER, M. An adaptability limit to climate change due to heat stress. **Proceedings of the National Academy of Sciences**. v. 107, n. 21, p. 9552–9555, Mar. 2010. DOI: https://doi.org/10.1073/pnas.0913352107.

SILVA, F. T.; ALVAREZ, C. E. An integrated approach for ventilation's assessment on outdoor thermal comfort. **Building and Environment**, v. 87, p. 59-71, May 2015. DOI: https://doi.org/10.1016/j.buildenv.2015.01.018.

SULLIVAN, J.; SANDERS, L. D. **Method for obtaining wet-bulb temperature by modifying the psychrometric formula.** Washington: Center for Experiment Design and Data Analysis: National Oceanic and Atmospheric Administration (NOAA). 1974. Disponível em: https://repository.library.noaa.gov/view/noaa/1388/noaa_1388_DS1.pdf. Acesso em: 21 mai 2021.

THORSSON, S.; RAYNER, D.; PALM, G.; LINDBERG, F.; CARLSTRÖM, E.; BÖRJESSON, M.; NILSON, F.; KHORRAM-MANESH, A.; HOLMER, B. Is physiological equivalent temperature (PET) a superior screening tool for heat stress risk than Wet-Bulb globe temperature (WBGT) index? Eight years of data from the Gothenburg half marathon. **British Journal of Sports Medicine**, v. 55, n. 1, 2020. DOI: https://doi.org/10.1136/bjsports-2019-100632.

TRIANA, M. A.; LAMBERTS, R.; SASSI, P. Should we consider climate change for brasilian social housing? Assessment of energy efficiency adaptation measures. **Energy and Buildings**, v. 158, p. 1379-1392, Jan. 2018. DOI: https://doi.org/10.1016/j.enbuild.2017.11.003.

WMO. WORLD METEOROLOGICAL ORGANIZATION. **State of the Global Climate 2020:** Provisional Report. Geneva: WMO, 2020. 38 p. Disponível em: https://library.wmo.int/doc_num.php?explnum_id=10444. Acesso em: 20 maio 2021.

1 **Layra Ramos Lugão**
Architect and Urban Planner. Master in Architecture and Urbanism at the Federal University of Espírito Santo. Volunteer researcher at the Planning and Projects Laboratory of the Federal University of Espírito Santo. Postal Address: Fernando Ferrari Ave., 514, Vitória, ES - Brazil, Zip Code 29075-910.

2 **Juliana Silva Almeida Santos**
Architect and Urban Planner. Master in Architecture and Urbanism from the Federal University of Espírito Santo. PhD in progress at the Federal University of Espírito Santo. Researcher at the Planning and Projects Laboratory of the Federal University of Espírito Santo. Postal Address: Fernando Ferrari Ave., 514, Vitória, ES - Brazil, Zip Code 29075-910.

3 **Anderson Azevedo Fraga**
Architect and Urban Planner. Master in Architecture and Urbanism from the Federal University of Espírito Santo. Postal Address: Fernando Ferrari Ave., 514, Vitória, ES - Brazil, Zip Code 29075-910.

4 **Edna Aparecida Nico Rodrigues**
Architect and Urban Planner. PhD in Architecture and Urbanism from the Universidad del Bio-Bio, Chile. Associate

Professor at the Federal University of Espírito Santo. Postal Address: Fernando Ferrari Ave., 514, Vitória, ES - Brazil, Zip Code 29075-910.

5 **Cristina Engel de Alvarez**
Architect and Urban Planner. PhD. in Architecture and Urbanism from the University of São Paulo. Full Professor at the Federal University of Espírito Santo. Postal Address: Fernando Ferrari Ave., 514, Vitória, ES - Brazil, Zip Code 29075-910.